

Photoinduced melting of superconductivity in the high- T_c superconductor $\text{La}_{2-x}\text{Sr}_x\text{CuO}_4$ probed by time-resolved optical and terahertz techniques

M. Beyer,¹ D. Stadter,¹ M. Beck,¹ H. Schafer,¹ V. V. Kabanov,^{2,3} G. Logvenov,^{4,5} I. Bozovic,⁴ G. Koren,⁶ and J. Demsar^{1,2,3}

¹*Physics Department, Center of Applied Photonics, University of Konstanz, DE-78457 Konstanz, Germany*

²*Complex Matter Department, Jozef Stefan Institute, Ljubljana, Slovenia*

³*Zukunftskolleg, University of Konstanz, DE-78457 Konstanz, Germany*

⁴*Brookhaven National Laboratory, Upton, New York 11973, USA*

⁵*Max-Planck Institute for Solid State Research, DE-70569, Stuttgart, Germany*

⁶*Physics Department, Technion, Haifa, IL-32000 Israel*

(Received 23 September 2010; revised manuscript received 1 February 2011; published 13 June 2011; corrected 30 June 2011)

The dynamics of depletion and recovery of a superconducting state in $\text{La}_{2-x}\text{Sr}_x\text{CuO}_4$ thin films is investigated utilizing optical pump-probe and optical pump-THz-probe techniques as a function of temperature and excitation fluence. The absorbed energy density required to suppress superconductivity is found to be about eight times higher than the thermodynamically determined condensation energy density and nearly temperature independent between 4 and 25 K. These findings indicate that, during the time when the superconducting state suppression takes place (≈ 0.7 ps), a large part (nearly 90%) of the energy is transferred to the phonons with energy lower than twice the maximum value of the superconducting gap and only 10% is spent on Cooper pair breaking.

DOI: [10.1103/PhysRevB.83.214515](https://doi.org/10.1103/PhysRevB.83.214515)

PACS number(s): 74.40.Gh, 78.47.J–, 74.25.Kc, 74.72.–h

I. INTRODUCTION

In the last decade or so, numerous real-time studies of carrier relaxation dynamics in cuprate superconductors have been performed utilizing pump-probe techniques. The initial studies were aimed at the understanding of relaxation^{1–9} and the interplay between the superconducting gap and the normal state pseudogap.^{10–13} Recently, however, several reports explored the dependence on excitation intensity of depletion of the superconducting state^{14–17} as well as of photoinduced structural dynamics¹⁸ and phase transitions.^{19,20}

It has been known since 1971 that an intense laser pulse can destroy the superconducting (SC) state nonthermally; the absorbed energy density is lower than the energy density required to heat up the sample to the critical temperature.²¹ The rapid development of stable amplified laser systems, producing optical pulses with sub-100-fs pulse duration, has enabled studies of dynamics of SC suppression in real time.²² This technique enables direct measurement of the SC condensation energy E_c (the difference in the free-energy density between the SC and normal states at zero temperature). If, following photoexcitation with a fs optical pulse, the absorbed energy remains in the electronic subsystem during the process of SC state destruction, the absorbed (optical) energy density required to suppress SC, E_{opt} , should be equal to E_c .²³ In conventional superconductors, E_c can be directly determined by measuring the thermodynamic critical magnetic field $B_c(0)$, where $E_c = B_c^2(0)/2\mu_0$. However, in high- T_c cuprate superconductors, the critical magnetic fields are very high and hardly accessible experimentally. To determine E_c in cuprates, the T dependence of the electronic specific heat $C_e(T)$ has been studied.^{24,25} However, since $C_e(T)$ is determined by measuring the total specific heat of the SC sample, and subtracting the phonon part (obtained by measuring the specific heat of an impurity-doped non-SC sample), it may be prone to some uncertainty.

In a recent optical pump-probe (OPP) study, an attempt was made to determine E_c in single crystals of high-temperature superconductor $\text{La}_{2-x}\text{Sr}_x\text{CuO}_4$ (LSCO) by means of ultrafast optics.¹⁴ E_{opt} was found to be about one order of magnitude higher than the thermodynamically determined E_c .²⁵ This large difference can hardly be attributed to the experimental uncertainties, so it was concluded that the major part of E_{opt} is transferred to the phonon subsystem on the sub-picosecond time scale.¹⁴ Indeed, a recent optical pump-THz-probe (OPTP) study in optimally doped $\text{YBa}_2\text{Cu}_3\text{O}_{7-\delta}$ (YBCO) (Ref. 16) showed rapid heating of the two infrared-active c -axis phonon modes on the time scale of 150 fs.¹⁶ Moreover, E_{opt} was also found to be about 10 times larger than E_c .¹⁶ Similar studies on $\text{Bi}_2\text{Sr}_2\text{CaCu}_2\text{O}_{8+\delta}$ (Bi2212) single crystals^{15,17,26} also indicate that $E_{\text{opt}} \approx 10E_c$.

Here we report the results of the study of $\text{La}_{2-x}\text{Sr}_x\text{CuO}_4$ ($x = 0.08, 0.16, 0.21$) thin films using both OPP and OPTP. In addition to the low-temperature measurements, the temperature dependence of E_{opt} was studied. We find that, within the experimental uncertainty, both OPP and OPTP give an identical value of E_{opt} for LSCO. This observation is of particular importance, since OPTP is probing the gap resonantly. The obtained value of E_{opt} is nearly identical to the one extracted from the OPP studies on LSCO single crystals.¹⁴ In addition, we find almost no temperature dependence of E_{opt} below T_c . This observation, together with the fact that $E_{\text{opt}} \approx 8E_c$, strongly suggests that during the time when the SC state suppression takes place, most of the absorbed energy is transferred to phonons with energy lower than 2Δ , where Δ denotes the value of the SC gap maximum. Because of strong reduction in the density of states at low energies in d -wave superconductors, Cooper pair breaking by phonons with $\hbar\omega < 2\Delta$ is strongly suppressed. In LSCO, about 90% of the absorbed energy is directly released to the lattice due to strong e - ph relaxation and only $\sim 10\%$ is spent on destruction of the condensate (Cooper pair breaking).

II. EXPERIMENT

The LSCO thin films used in this study were grown on LSAO substrate either by molecular beam epitaxy²⁷ (MBE) or by pulsed-laser deposition (PLD).²⁸ The film grown by MBE ($x = 0.16$) had a thickness of 52 nm with surface roughness less than one monolayer, and exhibited a critical temperature T_c of 31 K. The films grown by PLD ($x = 0.08, 0.21$) were 75 ± 5 nm thick with surface roughness of about 2 nm, and T_c 's of 22 and 25 K, respectively. The OPP experiments were performed in a high-sensitivity pump-probe setup utilizing a 250-kHz regenerative Ti:sapphire amplifier, delivering 50-fs pulses at 800 nm (1.55 eV), and a fast-scan technique.²⁹ The pump and probe beam diameters were measured accurately with a CCD camera, and were 120 and 60 μm , respectively, to ensure a homogeneous excitation profile. The OPTP experiments were performed using a setup based on the same amplifier system, employing a large-area photoconductive finger emitter generating phase-locked THz pulses with spectrum covering 0.2–3 THz range.³⁰ The THz beam was focussed to about 1.5 mm, while the pump beam diameter was about 3 mm, to ensure a homogeneous excitation profile. Experiments were conducted in a wide range of excitation fluences (3 orders of magnitude), spanning from $F = 0.1 \mu\text{J}/\text{cm}^2$ up to 200 (100) $\mu\text{J}/\text{cm}^2$ in the OPP (OPTP) configurations.

III. RESULTS

Figure 1 presents the photoinduced (PI) dynamics probed by the OPP and OPTP configurations at 4 K. The PI reflectivity ($\Delta R/R$) traces for different excitation fluences (in $\mu\text{J}/\text{cm}^2$) are shown in Fig. 1(a). As in many cuprate superconductors,^{4,12,13} two distinct relaxation components are observed in time-domain studies in LSCO, one (A) being present only below the SC critical temperature, while the other one (B) being sensitive to the opening of the normal state pseudogap.^{13,14} At low temperatures and excitation densities, the component A is dominant.¹³ It is characterized by a rise-time of ≈ 0.7 ps and the decay time on the 10-ps time scale. The component B, on the other hand, is characterized by a sub-100-fs rise-time and the recovery that is weakly dependent on temperature and excitation fluence, with the recovery time scale not exceeding 1 ps. Upon increasing the excitation fluence F , the component A shows saturation [see Fig. 2(a)], while the component B increases linearly with F up to much higher fluences. Given the fact that the component A can be attributed to suppression and recovery of the superconducting gap, its saturation observed at high excitation densities can be naturally attributed to the complete destruction of superconductivity.

To measure the dynamics of SC suppression and recovery in the THz range, over a large range of F , we have performed studies of the spectrally integrated conductivity change (often referred to as a one-dimensional scan technique).³¹ Here, the photoinduced change in the optical conductivity $\Delta\sigma$ is proportional to the photoinduced change in the transmitted electric field $\Delta E_{\text{tr}}(t' = t_0)$, where t_0 is a fixed point of $E_{\text{tr}}(t')$ trace [see the inset to Fig. 1(b)]. In LSCO, $2\Delta \gg 1$ THz, so the SC-induced change in the THz optical conductivity modifies the transmitted electric field transient mainly because of the appearance of the so-called kinetic inductance.²² To achieve

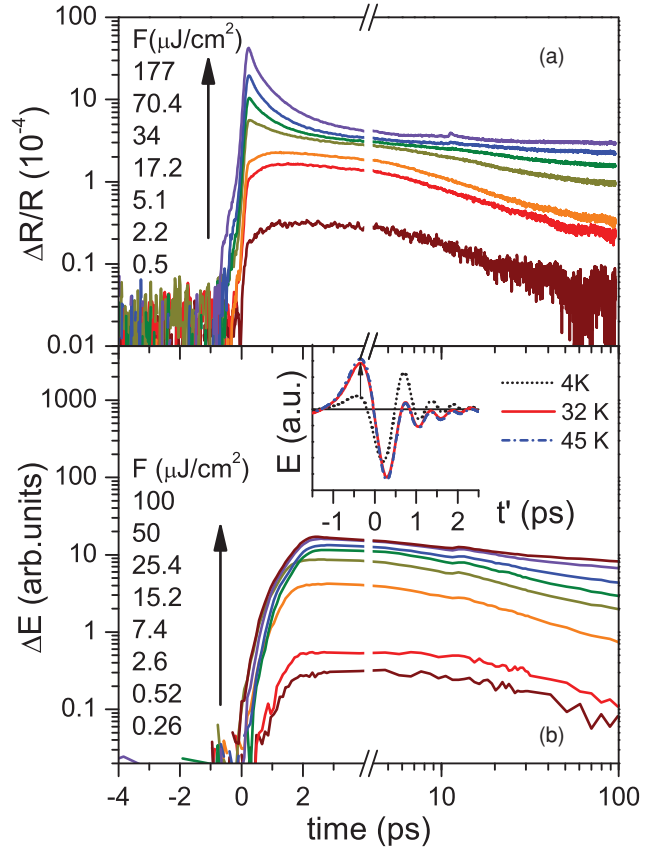


FIG. 1. (Color online) (a) PI reflectivity dynamics in $\text{La}_{1.84}\text{Sr}_{0.16}\text{CuO}_4$ at 4 K as a function of excitation fluence. (b) The corresponding dynamics of the PI change in the transmitted THz electric field. Inset: The THz electric field transient transmitted through the LSCO film on LSAO substrate at different temperatures. The arrow marks the t' , where the largest change between the SC and normal state is observed. The transients were shifted to 0 ps for display.

a high dynamic range, $\Delta E_{\text{tr}}(t_0 = -0.35 \text{ ps})$ was recorded [marked by an arrow in inset to Fig. 1(b)], where the change in the electric field transmitted through the sample ΔE_{tr} , corresponding to the transition between the SC and normal states, is the highest. The PI traces recorded in near optimally doped sample ($\text{La}_{1.84}\text{Sr}_{0.16}\text{CuO}_4$) at 4 K and at various fluences are displayed in Fig. 1(b). Similar to the component A from the OPP data, the amplitude of the induced change initially increases linearly with F and shows saturation at high F , as shown in Fig. 2(b).

Another noteworthy feature of the data shown in Fig. 1 is the dependence of the recovery dynamics on fluence. At lowest excitation densities, the PI changes in reflectivity and, in THz conductivity, almost completely recover, with the characteristic decay time of ≈ 10 ps (using the exponential decay fit). At higher excitation fluences, after the initial recovery on the 10-ps time scale, the induced change reaches a plateau, with further recovery proceeding on a much longer time scale. As we discuss below, this plateau can be attributed to an overall increase in the film temperature, and its recovery is governed by the heat diffusion to the substrate. Indeed, as the excitation density is increased above $\approx 50 \mu\text{J}/\text{cm}^2$, the

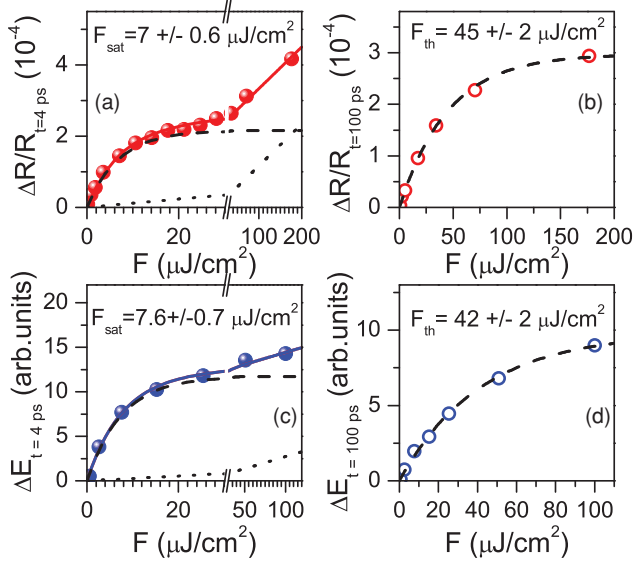


FIG. 2. (Color online) The evolution of the PI change in reflectivity at time delay (a) 4 ps and (b) 100 ps as a function of excitation density obtained at 4 K in the OPP configuration. The corresponding evolutions of the PI change in the THz electric field at t' obtained in the OPTP experiment are shown in (c) and (d). The data can be well fit with the simple saturation model (solid line, see text); long-dashed and short-dashed lines represent the first and second terms, respectively, of the the fit model. The fluence required to transiently suppress superconductivity is given by F_{sat} , while F_{th} matches well the fluence required to thermally heat up the sample to above T_c .

PI signal at the time delay of 100 ps, which is much longer than the characteristic SC state recovery time of ≈ 10 ps, also shows a saturation behavior [see Figs. 2(c) and 2(d)].

In Fig. 2(a), we plot the F dependence of the magnitude of component A, which is related to SC state suppression. In order to avoid picking up the contribution from component B, which starts to dominate once the component A saturates, we plot the magnitude of the signal at the time delay of 4 ps. To determine the characteristic fluence required to suppress SC, we use a simple saturation model

$$\Delta R/R(4 \text{ ps}) = C[1 - \exp(-F/F_{\text{sat}})] + DF. \quad (1)$$

The first term corresponds to the saturating part, where F_{sat} is the excitation fluence required to suppress the SC. The second term in Eq. (1) is accounting for small contribution from the component B, which at high F is not negligible despite the fact that the recovery time of component B is less than 1 ps. C and D are constants. From the best fit to the data [solid curve in Fig. 2(a)], we obtain $F_{\text{sat}} = 7 \pm 0.6 \mu\text{J}/\text{cm}^2$. In Fig. 2(c), we plot the F dependence of the corresponding induced change in the transmitted THz electric field $\Delta E_{\text{tr}}(t_0)$, again recorded at 4 ps after photoexcitation. Similar to the OPP data, the saturation of the induced change is observed with $F_{\text{sat}} = 7.6 \pm 0.7 \mu\text{J}/\text{cm}^2$. Within the uncertainty in the absolute excitation densities in the two configurations, the values for F_{sat} obtained in the two experimental configurations are identical.

To accurately determine the absorbed energy density, which corresponds to the optically induced suppression of

the SC state, we have measured the dielectric constants of $\text{La}_{2-x}\text{Sr}_x\text{CuO}_4$ at the excitation photon energy of 1.55 eV (800 nm). By measuring the reflectivity R and transmission T through the film on substrate and through the bare substrate, and using the appropriate Fresnel equations, we numerically solved a system of equations for R and T .³² The extracted complex refractive index of $\text{La}_{1.84}\text{Sr}_{0.16}\text{CuO}_4$ is $\tilde{n}(800 \text{ nm}) = n + ik = 2.06 + i0.38$. From the measured reflectivity and the extinction coefficient ($\alpha = 5.8 \times 10^4 \text{ cm}^{-1}$), we obtained the absorbed energy density that corresponds to F_{sat} and E_{opt} . For near optimally doped $\text{La}_{1.84}\text{Sr}_{0.16}\text{CuO}_4$, $E_{\text{opt}} \approx 0.35 \text{ J cm}^{-3}$, which corresponds to 2.4 $k_B\text{K}$ per Cu atom (i.e., $E_{\text{opt}} \approx 2.4 \text{ K/Cu}$).

In Figs. 2(b) and 2(d), we plot the F dependence of the PI change in reflectivity and in the transmitted THz electric field, at the time delay of 100 ps. Since this is substantially longer than the time scale for SC recovery, we can assume that 100 ps after photoexcitation the film is in the quasiequilibrium, where the electronic system and the underlying lattice are thermalized at a given temperature. Similar to the PI amplitude at short time delays, the saturation of the signal is observed with a characteristic fluence $F_{\text{th}} \approx 40\text{--}45 \mu\text{J}/\text{cm}^2$, which corresponds to the absorbed energy density $E_{\text{th}} \approx 2 \text{ J cm}^{-3} = 13.7 \text{ K/Cu}$.

We should note that, in our case, the excitation density is nearly homogeneous throughout the probed volume since (i) the pump spot diameter is twice bigger than the probe spot diameter and (ii) the film thickness (52 or 75 nm) is substantially lower than the optical penetration depth [e.g., $l_{\text{opt}}(\text{La}_{1.84}\text{Sr}_{0.16}\text{CuO}_4) = 170 \text{ nm}$]. Thus, the values for E_{opt} and E_{th} are quite precise.

The absorbed energy density corresponding to transiently suppressing the SC state E_{opt} is about eight times higher than $E_c \approx 0.3 \text{ K/Cu}$.²⁵ On the other hand, E_{opt} is by about a factor of 5 to 6 lower than the energy required to heat up the excited sample volume to above T_c . Using the reported data on the total specific heat for the optimally doped LSCO,³³ we obtain $U_{\text{th}} = \int_4^T C_p(T) dT \approx 1.6 \text{ J cm}^{-3} \approx 11 \text{ K/Cu}$. This value is in very good agreement with $E_{\text{th}} \approx 13.7 \text{ K/Cu}$, implying that, at fluences above F_{th} , superconductivity is also thermally suppressed, with its recovery proceeding on the time scale determined by the heat diffusion. The excellent agreement between E_{opt} obtained by OPP and OPTP techniques, as well as the agreement between E_{th} and U_{th} , strongly indicate that $E_{\text{opt}} \approx 8E_c$, where E_c is determined thermodynamically.

To gain further insight into the energetics of the photoinduced SC to normal phase transition, we have performed temperature-dependent studies of photoinduced quenching of superconductivity. Importantly, continuous heating of the sample is (in the case of thin films) substantially reduced in comparison to single crystals since the low-temperature thermal conductivity of LSAO substrate³⁴ is much higher than that of LSCO (especially in the c direction).³⁵ Therefore, the cumulative temperature increase of the probed spot is negligible, enabling such studies all the way up to close vicinity of T_c . In Fig. 3, we present the F dependence of PI reflectivity change at time delay of 4 ps, recorded in near optimally doped LSCO at several temperatures below and above $T_c = 31 \text{ K}$.

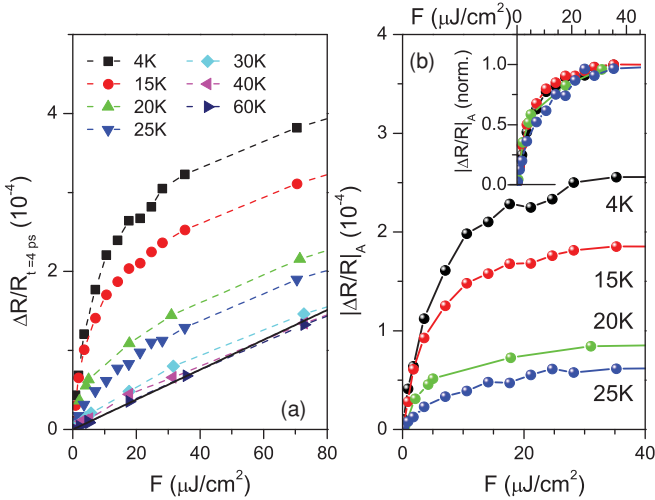


FIG. 3. (Color online) (a) The fluence dependence of the PI change at 4-ps time delay recorded in $\text{La}_{1.84}\text{Sr}_{0.16}\text{CuO}_4$ at different temperatures. From $T_c = 31$ to 60 K, all the data fall on the single curve, showing linear fluence dependence of the signal within the range of fluences studied. By subtracting this temperature-independent linear term (stemming from component B) from the data recorded at different T , we obtain the F dependence of the component A [shown in panel (b)]. The threshold fluence F_{sat} is found to be nearly T independent, as demonstrated by normalizing all the curves (see inset).

Above T_c , all the data fall on the same curve, displaying linear F dependence of the normal state response. Below T_c , the signal clearly shows two contributions, one (A) showing saturation above F_{sat} , while the other (B) showing linear F dependence, with the slope being T independent in the range of temperatures studied. By subtracting the contribution of the component B from all the data, we obtain the fluence dependence of the component A [see Fig. 3(b)]. Interestingly, F_{sat} (E_{opt}) is found to be nearly temperature independent up to 25 K.

Similar data to that on a near optimally doped film (Fig. 3) were obtained also in an underdoped $x = 0.08$ and an overdoped $x = 0.21$ film prepared by pulsed-laser deposition. Figure 4 summarizes the results on an $x = 0.08$ sample in the optical pump-probe configuration (similar data are obtained in the optical pump-THz-probe configuration). Also, in the normal state, the photoinduced reflectivity change varies linearly with fluence (component B). When the normal state response is subtracted from the data, the superconducting response (component A) shows clear saturation [Fig. 4(b)], with the threshold fluence F_{sat} required to transiently suppress superconductivity being nearly temperature independent all the way to $T_c = 22$ K.

Figure 5 summarizes the values of the E_{opt} for various dopings obtained in $\text{La}_{2-x}\text{Sr}_x\text{CuO}_4$ thin films together with the values obtained on the single crystals.¹⁴ For all films, the values of the complex refractive index were determined by measuring reflectivity and transmission at near normal incidence through the film and the bare substrate and numerical analysis of Fresnel equations.³² The larger error bars on films grown by pulsed-laser deposition stem from the uncertainty in the film thickness of ± 5 nm.

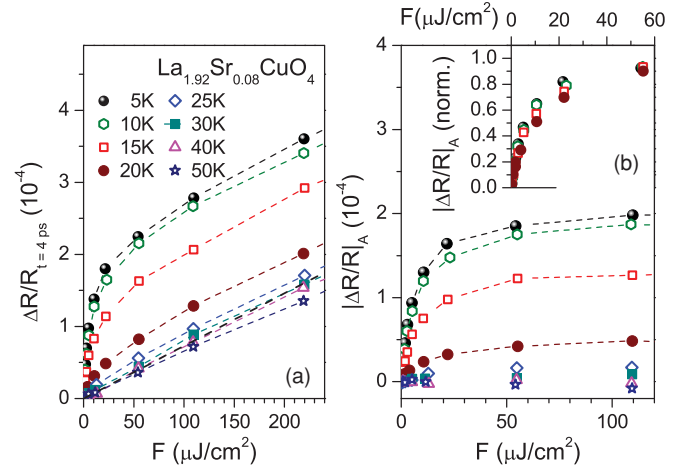


FIG. 4. (Color online) (a) The evolution of the PI change in reflectivity at a time delay of 4 ps in $\text{La}_{1.92}\text{Sr}_{0.08}\text{CuO}_4$ film recorded at different temperatures. As in the case of the near optimally doped film ($x = 0.16$), above T_c (24 K) all the data fall on the single curve, showing linear fluence dependence (due to component B). (b) When the linear in F contribution is subtracted from the data, only the part showing saturation (component A) remains. The inset shows the normalized F dependence of component A, demonstrating the absence of T temperature of F_{sat} (E_{opt}).

IV. DISCUSSION

The observation of E_{opt} being nearly T independent below T_c with $E_{\text{opt}}/E_c \approx 8$ is in striking contrast to similar studies on the NbN superconductor.³⁶ There, E_{opt} was found³⁶ to be equal to E_c , with both following the temperature dependence of Δ^2 . The large disproportionality between the E_{opt} and E_c was argued¹⁴ to be due to transfer of a large fraction of the absorbed optical energy to high-frequency ($\hbar\omega > 2\Delta$) phonons on the time scale required to suppress superconductivity (≈ 0.7 ps in LSCO). On the other hand, in conventional superconductors such as MgB_2 (Ref. 22) and NbN,³⁶ the optically induced suppression of the SC state also takes place via a two-step

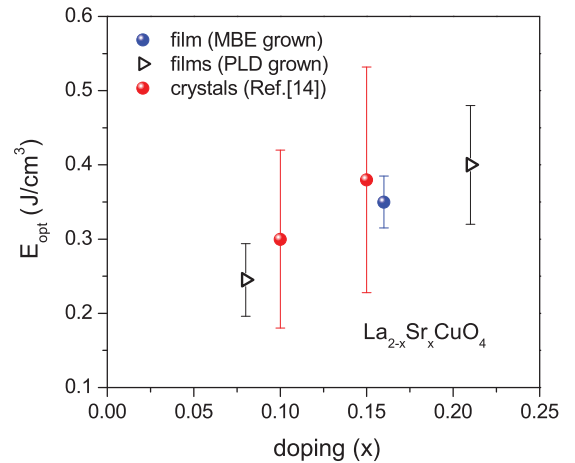


FIG. 5. (Color online) Doping dependence of E_{opt} in $\text{La}_{2-x}\text{Sr}_x\text{CuO}_4$, combining the results obtained on thin films with those obtained in single crystals (Ref. 14).

process.²² Here, high-energy electrons (holes) created by absorption of photons with energy much larger than the gap energy first relax toward the gap via $e-e$ and $e-ph$ scattering. The fact that the pair-breaking time (≈ 10 ps) is large and excitation-density dependent²² was attributed to the fact that, during the initial $e-e$ and $e-ph$ scattering, a high density of optical phonons with energies larger than 2Δ is generated, which subsequently break Cooper pairs⁹ on the 10-ps time scale. The question arises, then, as to why $E_{\text{opt}}/E_c \approx 8$ in LSCO and YBCO, while $E_{\text{opt}} \simeq E_c$ in NbN. To answer this question, we discuss the nature of $e-ph$ scattering processes and compare the phonon spectra and sizes of the superconducting gaps Δ between the two cases.

As it was pointed out also in Ref. 37, the dominant process in cooling of photoexcited electrons (holes) is the inelastic scattering by phonons; $e-e$ scattering is dominant only if the energy of the electron (hole) is far from the Fermi energy. Here, we would like to address the issue of the energy and momentum distributions of phonons generated by hot electrons (holes). Generally, the transition rate of the electron with momentum \mathbf{k} and energy $\epsilon_{\mathbf{k}} = \hbar^2 k^2/2m$ to the state with the momentum $\mathbf{k}' = \mathbf{k} + \mathbf{q}$ via emission of a phonon with the momentum \mathbf{q} and frequency ω is given by

$$w_q = \frac{2\pi}{\hbar} |M_{\mathbf{q}}|^2 (N_{\mathbf{q}} + 1) [1 - n(\epsilon_{\mathbf{k}-\mathbf{q}})] \delta(\epsilon_{\mathbf{k}} - \epsilon_{\mathbf{k}-\mathbf{q}} - \hbar\omega), \quad (2)$$

where $M_{\mathbf{q}}$ is the matrix element that depends on the $e-ph$ scattering mechanism, while $N_{\mathbf{q}}$ and $n(\epsilon_{\mathbf{k}-\mathbf{q}})$ are the equilibrium distribution functions of phonons and electrons, respectively. By integrating Eq. (2) over $\frac{d^3 q}{(2\pi)^3}$, one obtains the number of phonons generated by a hot electron (or hole) per unit of time. Note that this expression represents only one part of the $e-ph$ collision integral.³⁷ The second part describes the phonon absorption (mainly Cooper pair breaking), which is strongly energy dependent in the case of a superconductor with the gap in the quasiparticle excitation spectrum. Frequently, one is not interested in the momentum distribution of phonons and electrons and considers their distribution as a function of energy only. However, here one should consider also the momentum distribution of generated phonons. To find the rate of generation of phonons at a particular wave vector $q = |\mathbf{q}|$, we integrate the expression (2) over the angular part of \mathbf{q} , keeping the modulus of q constant. Since experiments are performed at low temperatures and rather low excitation densities, we can assume that $N_{\mathbf{q}} \approx n(\epsilon_{\mathbf{k}-\mathbf{q}}) \approx 0$. Under this assumption, we obtain

$$w_q = \frac{(2\pi)^2 |M_{\mathbf{q}}|^2 m}{\hbar^3 k q}, \quad (3)$$

where m is the effective mass of charge carriers. Equation (3) describes the phonon generation rate by hot electrons (holes). For metals, we can substitute k in Eq. (3) by the Fermi wave vector k_F , assuming a large Fermi energy. Because of the energy conservation $\hbar^2 \mathbf{k}^2/2m - \hbar^2 (\mathbf{k} - \mathbf{q})^2/2m = \hbar\omega$ and momentum conservation, the phonon wave vector in Eq. (3) is restricted by $q_{\text{min}} < q < q_{\text{max}}$, where $q_{\text{min}} \approx m\omega/\hbar k_F$ and $q_{\text{max}} \approx 2k_F$.

In most metals, screening is strong, and the matrix element of the electron interaction with optical phonons [deformation

optical phonon scattering (DO)] is³⁸ momentum independent $|M_q^{\text{DO}}|^2 = \text{const}$. Since $w_q^{\text{DO}} \propto 1/q$ [see Eq. (3)], generation of optical phonons at $q \approx q_{\text{min}}$ is dominant. Yet, since the phase volume of $q \approx q_{\text{min}}$ phonons is small, when we integrate Eq. (3) with $q^2 dq/(2\pi)^3$, the total energy accumulated by the low- q optical phonons remains small.

The matrix element of the interaction of electrons with acoustic phonons [deformation acoustic phonon scattering (DA)] has $|M_q^{\text{DA}}|^2 \propto q$ dependence,³⁸ and thus w_q^{DA} is momentum independent; hence, the energy is mainly transferred to the high- q (high- ω) acoustic phonons due to their large phase volume.

In NbN, the phonon spectrum consists of acoustic branches extending up to ≈ 28 meV and the weakly dispersing optical branches at ≈ 60 meV,³⁹ while $2\Delta = 6$ meV.⁴⁰ From the above considerations, it follows that the initial $e-ph$ scattering process generates a high density of optical phonons and high-frequency acoustic phonons, all of which have energy larger than 2Δ . All of these phonons can effectively break Cooper pairs. When, on the time scale of Cooper pair breaking (≈ 10 ps in NbN), the quasiequilibrium is established between the populations of quasiparticles and phonons with $\hbar\omega > 2\Delta$, the excess energy is almost exclusively stored in the electronic subsystem.^{9,41} Therefore, it is no surprise that $E_{\text{opt}} \simeq E_c$, as experimentally observed.

In high- T_c superconductors, however, in addition to the DO and DA processes, the scattering on the c -axis polar (infrared-active) optical phonons [polar optical scattering (PO)] is possible. Since the c -axis plasma frequency is low, the polar optical phonons are unscreened.⁴² As it is well known,³⁸ the matrix element of the interaction of electrons with polar optical phonons scales as $|M_q^{\text{PO}}|^2 \sim 1/q^2$. Since $w_q^{\text{PO}} \propto 1/q^3$, the nonequilibrium distribution function of polar c -axis phonons is strongly peaked at low q . Moreover, in the case of PO, the integration over the phase volume does not cancel the $1/q^3$ dependence of the generation rate. Therefore, for scattering on polar optical phonons, also most of the energy is accumulated near the Γ point of the Brillouin zone, and it can be sizable, as demonstrated.¹⁶

In LSCO, acoustic branches extend up to ≈ 10 meV, while the spectrum of optical phonons continuously extends all the way to 100 meV with a maximum in the phonon density of states near 20–30 meV.⁴³ On the other hand, in LSCO, the value of the gap maximum in the antinodal direction is⁴⁴ $\Delta \approx 15$ meV. Comparison of $2\Delta \approx 30$ meV with the phonon density of states, taking into account the different $e-ph$ scattering mechanisms, reveals that in LSCO the $e-ph$ scattering creates a high density of phonons with $\hbar\omega < 2\Delta$. The Cooper-pair-breaking process by absorption of phonons with $\hbar\omega < 2\Delta$ is strongly suppressed even in d -wave superconductors due to the energy and momentum conservation laws and the strong reduction in the density of states at low energies.⁴⁵ Therefore, the generation of phonons with $\hbar\omega < 2\Delta$ can present a parallel energy relaxation channel, competing with Cooper pair breaking. Since $\Delta(T)$ does not change substantially between 4 K and $0.8 T_c$, it is conceivable that relaxation via these channels is the cause of the observed large difference between E_{opt} and E_c .

The calculation of phonon emission rates for various possible e - ph scattering processes is generally difficult and clearly beyond the scope of this paper. However, for the generation of c -axis polar modes via the polar optical phonon scattering, such a calculation is rather straightforward and can be directly compared with the recent studies of time-resolved c -axis THz conductivity dynamics in the superconducting state of YBCO.¹⁶ In this paper, in addition to the quasi-particle (QP) relaxation dynamics, the dynamics of two infrared-active phonons has been investigated, showing a remarkably fast increase in the phonon population density of the apical phonon on the time scale of ≈ 150 fs.¹⁶ By integrating Eq. (3) with $q^2 dq / (2\pi)^3$ and taking into account that $|M_q^{\text{PO}}|^2 = \frac{1}{4\pi\epsilon_0} \frac{2\pi e^2 \omega}{\kappa q^2}$, where $\kappa^{-1} = \epsilon_\infty^{-1} - \epsilon_0^{-1}$ and $\epsilon_0, \epsilon_\infty$ are the static and the high-frequency dielectric functions, respectively, we obtain [see also Eq. (4.53) in Ref. 38]

$$\tau^{-1} = \frac{1}{4\pi\epsilon_0} \frac{me^2\omega}{\hbar^2\kappa k_F} \ln(q_{\text{max}}/q_{\text{min}}), \quad (4)$$

where ϵ_0 is the permittivity of vacuum. By using the values for the c -axis dielectric constants $\epsilon_0 \approx 30$, $\epsilon_\infty \approx 5$,⁴⁶ $k_F \sim \pi/a$ (where a is the lattice constant), and the free electron mass, we obtain $\tau \sim 5$ fs for the generation of one c -axis polar optical phonon with $\hbar\omega = 50$ meV. Therefore, in the absence of phonon reabsorption processes, the electron (hole) at $\epsilon = 1$ eV above (below) the Fermi energy releases its excess energy to c -axis polar optical phonons on the time scale of $\tau\epsilon/\hbar\omega = 100$ fs, consistent with measurements on YBCO.¹⁶ Indeed, the maximum photoinduced softening of the apical phonon in YBCO is comparable to the effect induced by a thermal phonon population at $T \approx 200$ K,¹⁶ suggesting that the phonon distribution function is, on the sub-picosecond time scale, highly nonthermal.

As we have shown, following absorption of high-energy photons, hot electrons (holes) in cuprate superconductors rapidly relax toward the gap energy by generating large densities of phonons (predominantly zone-edge acoustic and zone-center polar optical phonons). Since in cuprates (investigated to date) 2Δ is comparable to the phonon cutoff frequency, a large portion of the absorbed energy is on the 100-fs time scale transferred to $\hbar\omega < 2\Delta$ phonons without affecting superconductivity.

The doping-dependent study (see Fig. 5) reveals a nearly linear increase of E_{opt} as a function of doping. Qualitatively, the increase of E_{opt} from the strongly underdoped LSCO toward optimal doping could be understood within the above scenario to be a result of an increase in the gap energy scale and therefore the number of phonon modes with $\hbar\omega < 2\Delta$ upon doping. However, given the fact that Δ shows a decrease upon entering the overdoped range,^{47,48} one would expect E_{opt} to follow this dependence. The fact that E_{opt} shows no decrease in the overdoped regime, however, implies that the generation rate of $\hbar\omega < 2\Delta$ phonons is also affected by doping, increasing with x .

The question arises, however, as to whether the observation that the generation rate of $\hbar\omega < 2\Delta$ phonons is increasing with doping necessary means that the electron-phonon coupling constant λ is increasing with doping. The short answer is no. The dimensionless $e - ph$ coupling constant λ , which in the

BCS theory determines the value of the critical temperature, is defined as

$$\lambda = 2 \int_0^\infty d\omega \frac{\alpha^2 F(\omega)}{\omega}, \quad (5)$$

where $\alpha^2 F(\omega)$ is the Eliashberg function, which depends only on the phonon frequency ω . In general, however, the Eliashberg function depends also on the energy of electron. For simplicity, let us consider good metals, where screening is large and the momentum dependence of electron-phonon interaction becomes less important. In this case, according to Eq. (28) of Ref. 36, the relaxation of hot electrons can be described in terms of the Eliashberg function $\alpha^2 F(\omega, \xi)$, which depends both on phonon frequency as well as the electron energy ξ counted from Fermi energy E_F .^{37,49} Since the characteristic energy of electrons in the thermodynamic equilibrium is small (of the order of $k_B T \sim k_B T_c \ll E_F$), it is usually neglected in the Eliashberg function, which enters into Eq. (5), i.e., $\alpha^2 F(\omega, \xi \approx 0) = \alpha^2 F(\omega)$. However, after photoexcitation, the characteristic energy of hot electrons is sufficiently higher than ω . Since the phonon generation rate by hot electrons is proportional to the spectral function of the electron-phonon interaction,³⁷ neglecting the ξ dependence in the Eliashberg function may be incorrect. If the function $\alpha^2 F(\omega, \xi)$ at ξ of the order of the photon energy ξ_{ph} is sufficiently different from the Eliashberg function at $\xi = 0$, this can have a very strong effect on the optical energy required for the depletion of the superconducting state. For example, if hot electrons interact mainly with the low-frequency phonons [i.e., $\alpha^2 F(\omega, \xi_{ph})$ is peaked at low frequencies], while $\alpha^2 F(\omega, \xi = 0)$ is peaked in the range of high-frequency phonons, the initial relaxation of hot electrons may create phonons that do not interact with electrons at $\xi \sim T$ and do not give rise to Cooper pair breaking. In the opposite case, when hot electrons interact mainly with the high-frequency phonons, while $\alpha^2 F(\omega, \xi = 0)$ is peaked at low frequencies, the electrons near the Fermi energy are only weakly coupled to the high-frequency optical modes. In such a case, the optical phonons first need to decay into the low-frequency ones before Cooper pair breaking can take place, and the pair-breaking process will be strongly delayed.

From the experiments performed on cuprates thus far,¹⁴⁻¹⁷ the characteristic time scales for suppression of superconductivity are in the range of 100 to several hundred femtoseconds. From the above considerations, we suggest that, in cuprates, the dominant part of the absorbed energy is on the 100-fs time scale transferred to $\hbar\omega < 2\Delta$ phonons, which do not take part in the Cooper-pair-breaking process. To further clarify these interesting observations, systematic studies of the Cooper-pair-breaking process as a function of excitation photon energy, measuring both the dynamics of the condensate as well as that of the phonons,¹⁶ are required, some of which are already underway.

V. CONCLUSIONS

Utilizing optical pump-probe and optical pump-THz-probe techniques, we have performed systematic studies of the dynamics of suppression and recovery of the superconducting state in $\text{La}_{2-x}\text{Sr}_x\text{CuO}_4$ thin films. The results clearly demonstrate that the absorbed energy density required to

suppress superconductivity exceeds the thermodynamically determined condensation energy by a factor of ≈ 8 , yet this energy is by a factor of 5 to 6 lower than the energy required to thermally heat up the photoexcited volume to above T_c . While there is some uncertainty in the existing determination of the condensation energy, it could hardly explain the observed high E_{opt}/E_c ratio. Moreover, the lack of temperature dependence of E_{opt} up to $\approx 0.8 T_c$ clearly suggests that the measured $E_{\text{opt}} > E_c$, and suggests the existence of a parallel energy relaxation channel. By considering various e - ph scattering mechanisms, we conclude that, in $\text{La}_{2-x}\text{Sr}_x\text{CuO}_4$, a large amount of the absorbed optical energy is transferred to phonons with $\hbar\omega < 2\Delta$, on the 100-fs time scale. Since Cooper pair breaking by phonons with $\hbar\omega < 2\Delta$ is strongly suppressed, it is the e - ph scattering to $\hbar\omega < 2\Delta$ phonons that presents the parallel relaxation path.

From the available data on cuprate superconductors $\text{La}_{2-x}\text{Sr}_x\text{CuO}_4$ (this paper as well as Ref. 14), $\text{YBa}_2\text{Cu}_3\text{O}_{7-\delta}$,¹⁶ and $\text{Bi}_2\text{Sr}_2\text{CaCu}_2\text{O}_{8+\delta}$,^{15,17,26} it follows that the observed behavior may be a general feature of cuprate

superconductors. In all three cuprates studied thus far, E_{opt} was found to be about an order of magnitude larger than the thermodynamically determined condensation energy E_c , in contrast to the conventional superconductor NbN, where $E_{\text{opt}} \approx E_c$.³⁶ Clearly, further experiments, with photoexcitation photon energy tuned to the vicinity of 2Δ , are necessary to gain a deeper insight into the nature of the pair-breaking process in cuprates; some are already underway.

ACKNOWLEDGMENTS

J.D. acknowledges discussions with T. Dekorsy, A. Leitenstorfer, A. Pashkin, K. W. Kim, and P. Leiderer. The research was supported in parts by the Sofja-Kovalevskaja Grant from the Alexander von Humboldt Foundation, Zukunftskolleg, and CAP at the University of Konstanz, joint German-Israeli DIP Project (Grant No. 563363), and the Karl Stoll Chair in advanced materials (Technion). The work at BNL was supported by US DOE Contract No. MA-509-MACA.

-
- ¹S. G. Han, Z. V. Vardeny, K. S. Wong, O. G. Symko, and G. Koren, *Phys. Rev. Lett.* **65**, 2708 (1990).
- ²C. J. Stevens, D. Smith, C. Chen, J. F. Ryan, B. Podobnik, D. Mihailovic, G. A. Wagner, and J. E. Evetts, *Phys. Rev. Lett.* **78**, 2212 (1997).
- ³V. V. Kabanov, J. Demsar, B. Podobnik, and D. Mihailovic, *Phys. Rev. B* **59**, 1497 (1999).
- ⁴J. Demsar, B. Podobnik, J. E. Evetts, G. A. Wagner, and D. Mihailovic, *Europhys. Lett.* **45**, 381 (1999).
- ⁵G. P. Segre, N. Gedik, J. Orenstein, D. A. Bonn, R. Liang, and W. N. Hardy, *Phys. Rev. Lett.* **88**, 137001 (2002).
- ⁶M. L. Schneider *et al.*, *Eur. Phys. J. B* **36**, 327 (2003).
- ⁷R. D. Averitt, G. Rodriguez, A. I. Lobad, J. L. W. Siders, S. A. Trugman, and A. J. Taylor, *Phys. Rev. B* **63**, 140502(R) (2001).
- ⁸R. A. Kaindl, M. A. Carnahan, D. S. Chemla, S. Oh, and J. N. Eckstein, *Phys. Rev. B* **72**, 060510 (2005).
- ⁹V. V. Kabanov, J. Demsar, and D. Mihailovic, *Phys. Rev. Lett.* **95**, 147002 (2005).
- ¹⁰J. Demsar, B. Podobnik, V. V. Kabanov, T. Wolf, and D. Mihailovic, *Phys. Rev. Lett.* **82**, 4918 (1999).
- ¹¹R. A. Kaindl, M. Woerner, T. Elsaesser, D. C. Smith, J. F. Ryan, G. A. Farnan, M. P. McCurry, and D. G. Walmsley, *Science* **287**, 470 (2000).
- ¹²D. Dvorsek, V. V. Kabanov, J. Demsar, S. M. Kazakov, J. Karpinski, and D. Mihailovic, *Phys. Rev. B* **66**, 020510 (2002).
- ¹³P. Kusar, J. Demsar, D. Mihailovic, and S. Sugai, *Phys. Rev. B* **72**, 014544 (2005).
- ¹⁴P. Kusar, V. V. Kabanov, J. Demsar, T. Mertelj, S. Sugai, and D. Mihailovic, *Phys. Rev. Lett.* **101**, 227001 (2008).
- ¹⁵C. Giannetti, G. Zgrablic, C. Consani, A. Crepaldi, D. Nardi, G. Ferrini, G. Dhalenne, A. Revcolevschi, and F. Parmigiani, *Phys. Rev. B* **80**, 235129 (2009).
- ¹⁶A. Pashkin, M. Porer, M. Beyer, K. W. Kim, A. Dubroka, C. Bernhard, X. Yao, Y. Dagan, R. Hackl, A. Erb, J. Demsar, R. Huber, and A. Leitenstorfer, *Phys. Rev. Lett.* **105**, 067001 (2010).
- ¹⁷G. Coslovich, C. Giannetti, F. Cilento, S. Dal Conte, G. Ferrini, P. Galinetto, M. Greven, H. Eisaki, M. Raichle, R. Liang, A. Damascelli, and F. Parmigiani, *Phys. Rev. B* **83**, 064519 (2011).
- ¹⁸F. Carbone, D.-S. Yang, E. Giannini, and A. H. Zewail, *Proc. Natl. Acad. Sci. USA* **105**, 20161 (2008).
- ¹⁹N. Gedik, D.-S. Yang, G. Logvenov, I. Bozovic, and A. H. Zewail, *Science* **316**, 425 (2007).
- ²⁰Z. Radovic, N. Bozovic, and I. Bozovic, *Phys. Rev. B* **77**, 092508 (2008).
- ²¹L. R. Testardi, *Phys. Rev. B* **4**, 2189 (1971).
- ²²J. Demsar, R. D. Averitt, A. J. Taylor, V. V. Kabanov, W. N. Kang, H. J. Kim, E. M. Choi, and S. I. Lee, *Phys. Rev. Lett.* **91**, 267002 (2003); *Int. J. Mod. Phys. B* **17**, 3675 (2003).
- ²³E. J. Nicol and J. P. Carbotte, *Phys. Rev. B* **67**, 214506 (2003).
- ²⁴J. W. Loram, K. A. Mirza, J. R. Cooper, W. Y. Liang, and J. M. Wada, *J. Supercond.* **7**, 243 (1994).
- ²⁵T. Matsuzaki, N. Momono, M. Oda, and M. Ido, *J. Phys. Soc. Jpn.* **73**, 2232 (2004).
- ²⁶R. Cortes, L. Rettig, Y. Yoshida, H. Eisaki, M. Wolf, and U. Bovensiepen, e-print [arXiv:1011.1171v1](https://arxiv.org/abs/1011.1171v1).
- ²⁷I. Bozovic, G. Logvenov, M. A. J. Verhoeven, P. Caputo, E. Goldobin, and T. H. Geballe, *Phys. Rev. Lett.* **89**, 107001 (2002); I. Bozovic *et al.*, *Nature (London)* **422**, 873 (2003).
- ²⁸O. Yuli, I. Asulin, O. Millo, and G. Koren, *Phys. Rev. B* **75**, 184521 (2007).
- ²⁹A. Tomeljak, H. Schäfer, D. Städter, M. Beyer, K. Biljakovic, and J. Demsar, *Phys. Rev. Lett.* **102**, 066404 (2009); H. Schäfer, V. V. Kabanov, M. Beyer, K. Biljakovic, and J. Demsar, *ibid.* **105**, 066402 (2010).
- ³⁰M. Beck, H. Schäfer, G. Klatt, J. Demsar, S. Winnerl, M. Helm, and T. Dekorsy, *Opt. Express* **18**, 9251 (2010).
- ³¹Detailed spectrally resolved equilibrium and nonequilibrium THz conductivity dynamics will be presented elsewhere.
- ³²R. Harbecke, *Appl. Phys. B* **39**, 165 (1986).

- ³³K. Kitahara, M. Hoshino, K. Kodama, and M. Ozeki, *Jpn. J. Appl. Phys.* **26**, 1119 (1987).
- ³⁴D. T. Morelli, *J. Mater. Res.* **7**, 2492 (1992).
- ³⁵X. F. Sun, J. Takeya, S. Komiya, and Y. Ando, *Phys. Rev. B* **67**, 104503 (2003).
- ³⁶M. Beck, M. Klammer, S. Lang, P. Leiderer, V. V. Kabanov, G. N. Gol'tsman, and J. Demsar, e-print [arXiv:1102.5616v1](https://arxiv.org/abs/1102.5616v1).
- ³⁷V. V. Kabanov and A. S. Alexandrov, *Phys. Rev. B* **78**, 174514 (2008).
- ³⁸V. F. Gantmakher and Y. B. Levinson, *Carrier Scattering in Metals and Semiconductors*, Modern Problems in Condensed Matter Science (Elsevier Science, New York, 1987), Vol. 19.
- ³⁹A. N. Christensen, O. W. Dietrich, W. Kress, W. D. Teuchert, and R. Currat, *Solid State Commun.* **31**, 795 (1979).
- ⁴⁰K. E. Kornelsen, M. Dressel, J. E. Eldridge, M. J. Brett, and K. L. Westra, *Phys. Rev. B* **44**, 11882 (1991).
- ⁴¹To estimate the amount of energy in the high-frequency ($>2\Delta$) phonon subsystem, which is in the bottleneck case in the quasithermal equilibrium with the electronic subsystem, we evaluate the energy required to heat up the high-frequency phonon subsystem to T_c . This energy is negligible compared to E_{opt} in both NbN and LSCO.
- ⁴²C. Bernhard, R. Henn, A. Wittlin, M. Kläser, Th. Wolf, G. Müller-Vogt, C. T. Lin, and M. Cardona, *Phys. Rev. Lett.* **80**, 1762 (1998); M. Grüninger, D. van der Marel, A. A. Tsvetkov, and A. Erb, *ibid.* **84**, 1575 (2000); M. A. Quijada, D. B. Tanner, F. C. Chou, D. C. Johnston, and S.-W. Cheong, *Phys. Rev. B* **52**, 15485 (1995).
- ⁴³S. L. Chaplot, W. Reichardt, L. Pintschovius, and N. Pyka, *Phys. Rev. B* **52**, 7230 (1995).
- ⁴⁴A. Ino *et al.*, *Phys. Rev. B* **65**, 094504 (2002); Q. Zhang *et al.*, *Phys. C (Amsterdam)* **386**, 282 (2003).
- ⁴⁵P. C. Howell, A. Rosch, and P. J. Hirschfeld, *Phys. Rev. Lett.* **92**, 037003 (2004).
- ⁴⁶D. Reagor, E. Ahrens, S. W. Cheong, A. Migliori, and Z. Fisk, *Phys. Rev. Lett.* **62**, 2048 (1989); A. S. Alexandrov and A. M. Bratkovsky, *Phys. Rev. Lett.* **84**, 2043 (2000).
- ⁴⁷H. Takagi, T. Ido, S. Ishibashi, M. Uota, S. Uchida, and Y. Tokura, *Phys. Rev. B* **40**, 2254 (1989).
- ⁴⁸O. Yuli, I. Asulin, O. Millo, and G. Koren, *Phys. Rev. B* **75**, 184521 (2007).
- ⁴⁹P. B. Allen and B. Mitrovic, *Solid State Phys.* **37**, 1 (1982).